Icarus 198 (2008) 318–330

Contents lists available at ScienceDirect

Icarus

www.elsevier.com/locate/icarus

Reinterpretation of Tractus Fossae region as an asymmetric rift system on Mars

Mauro G. Spagnuolo [a,*], Patricio H. Figueredo [b], Victor A. Ramos [a]

[a] Laboratorio de Tectónica Andina, Departamento de Geología, FCEyN Universidad de Buenos Aires, Intendente Güiraldes 2160, C1428EHA Buenos Aires, Argentina
[b] Department of Geological Sciences, Arizona State University, Tempe, AZ, USA

ARTICLE INFO

Article history:
Received 16 January 2008
Revised 10 August 2008
Available online 12 September 2008

Keywords:
Mars
Tectonics
Earth
Terrestrial planets
Planetary dynamics

ABSTRACT

The Tractus Fossae region of Mars is a wide area dominated by grabens, normal faults and pit crater chains. In this work, based on previous studies on the area and the new interpretation of topographic data and morphological units based on images as a geologic framework we present a new insight on the origin of the graben structures as well as on the processes associated with the formation of the volcanic features. Here we propose a new model for this region, on the basis of new measurements of graben extension and geological interpretations, together with a reinterpretation of the stratigraphy and the geologic history of the area. Finally, it is postulated that this region underwent a tectonic regime analog to an asymmetric rift system on Earth.

1. Introduction

The Tractus Fossae region of Mars is located at the Tharsis volcanotectonic province just between two prominent bulges (Fig. 1). The northern area (Fig. 1a) is dominated by the Alba Patera volcano; the second and largest region (Fig. 1b) consists of the central Tharsis region, from 20° N to 50° S, which covers an area of approximately 10^7 km^2 (Smith et al., 1999). This study area is dominated by a group of north–south grabens in the western section and two volcanic structures (Ceraunius Tholus and Uranius Tholus) in the eastern section (Fig. 2). In this work, we analyze the structural evolution of Tractus Fossae and its relation with the surrounding units and compare to the Wernicke model for the formation of terrestrial rift systems. For planetary comparisons, it is possible to study regions that have similar formation processes and deformation history to the ones recognized on the Earth. Therefore, a comparative study of Earth leads to an understanding of the dynamics and evolution of geologic processes that occur in other areas of the Solar System.

We start this work with a short review of relevant previous works on the study area. We then synthesize the information in a coherent mechanical framework, and provide new extension values for the area based on geologic interpretation and not only in geometrical parameters. Finally we incorporate all the evidence in the context of an asymmetric rift model.

1.1. Previous works

Carr et al. (1973) and Carr (1974) mapped the linear structures as a fractured plains unit. In his geologic map of the MC-9 quadrant (Carr, 1975), suggested that Ceraunius and Uranius Tholi were formed by low viscosity lavas. Scott et al. (1981) assigned a wide range of geologic ages to the units, ranging from Hesperian to Amazonian. Scott and Tanaka (1986) recognized the volcanic structures in their map of the Western Hemisphere, without assigning ages to them. Greeley and Spudis (1981) made reference to the Uranius Group suggesting that Ceraunius and Uranius Tholi were domes, whereas Hodges and Moore (1994) considered them as shield volcanoes of basaltic composition. In a more recent work, Plescia (2000) studied this volcanic group, reaching the conclusion that effusive processes, with an important participation of pyroclastic ejecta, mainly formed these volcanoes during the Hesperian epoch.

There are several regional works that deal with the faulting of the area, including those by Plescia and Saunders (1982), Tanaka (1986, 1990), Scott and Tanaka (1986), and Plescia (1991). These authors concluded that the age of the structures in this region ranged from late Noachian to early Hesperian. In a more recent work, Anderson et al. (2001, 2004) assigned the faulting stage to an older age, being exclusively Noachian. In a more recent study, Borraccini et al. (2005) have studied the extension along the faults in this area, applying new techniques in order to perform detailed topographic profiles, but did not postulate a mechanism by which this fault system could have been developed.

1.2. Geological setting

The volcanic edifices of Ceraunius and Uranius Tholi dominate the topographic relief in the study area. Hypsometric curves show

* Corresponding author.
E-mail address: mauro@gl.fcen.uba.ar (M.G. Spagnuolo).

0019-1035/$ – see front matter
doi:10.1016/j.icarus.2008.08.007

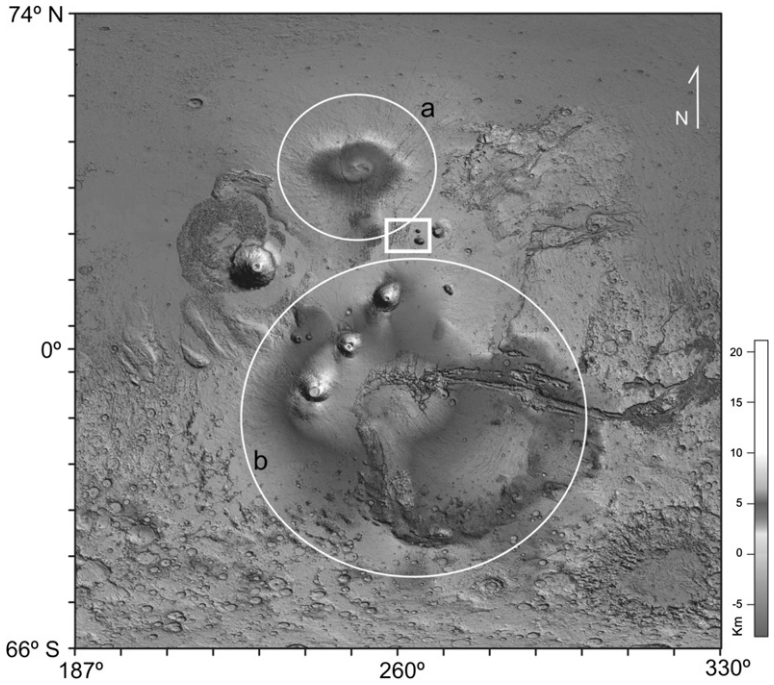

Fig. 1. Shaded relief image derived from MOLA data, with location of the study area (box) between the two prominent bulges (circles) on Tharsis region: (a) Alba Patera volcano to the north, and (b) Volcano complex which includes Acraeus, Pavonis and Arsia Mons to the south.

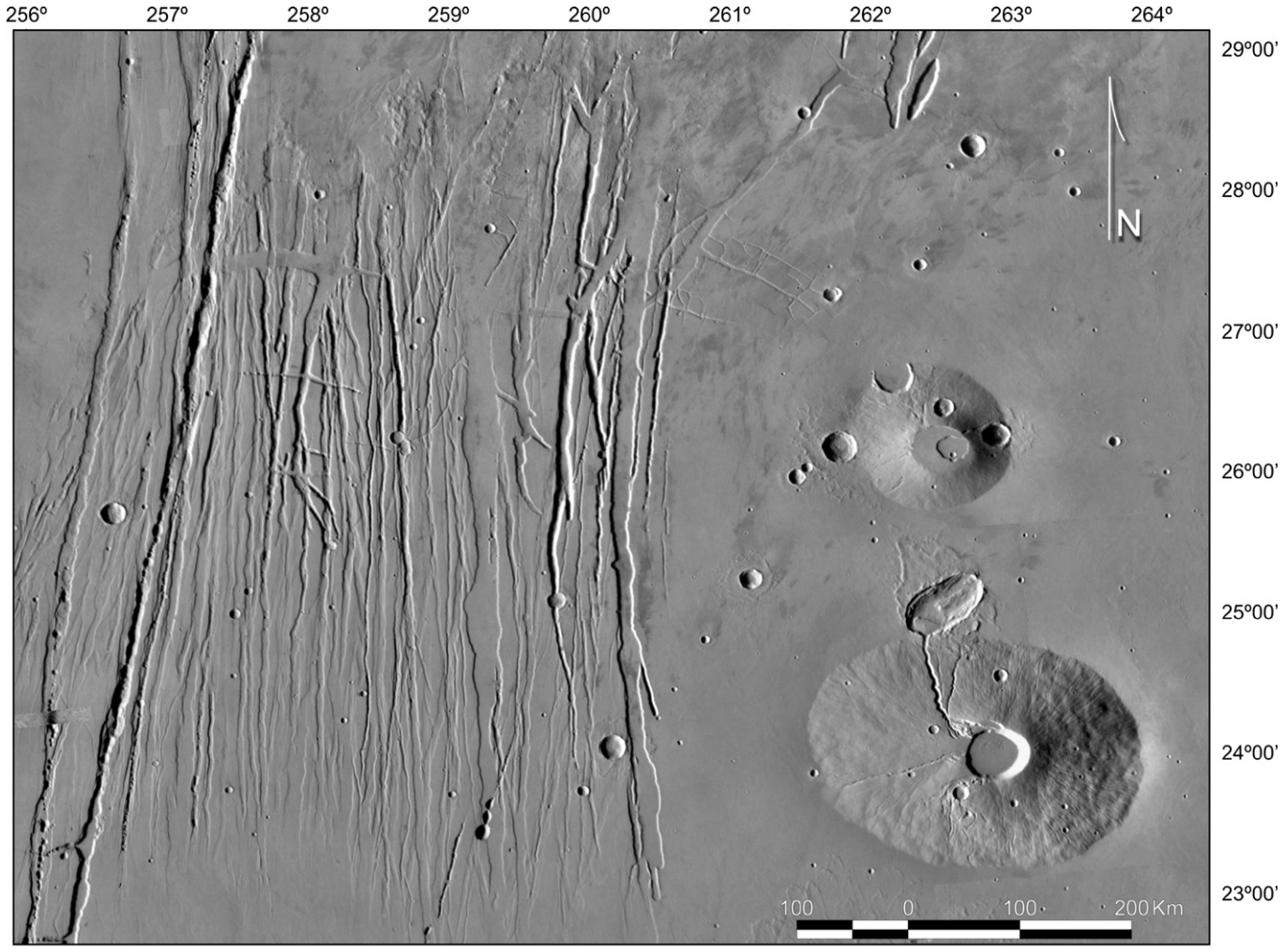

Fig. 2. MDIM 2.1 image map showing the study area. It can be observed the highly fractured terrain on the western section while lava plains and Uranius Tholus (north) and Ceraunius Tholus (south) volcanic edifices dominate the eastern sector, reaching 3 and 6 km respectively.

that almost 90% of the terrain is less than 2500 m high whereas 10% rises from 3000 up to 8500 m altitude. The elevated, faulted area of Tractus Fossae lies towards the west of the volcanic edifices. This zone occupies a total of approximately 71,610 km^2 and in its central part it rises near 500 m above surrounding plains. Most of the grabens display a north–south trend (Fig. 2) and their widths vary between 0.8 and 9 km. Borraccini et al. (2005) studied the relationship between the width and depth of these structures and concluded that there are two independent parameters, whereas the graben width is mostly controlled by rheology and the graben depth is mostly controlled by fault mechanics. In the western section, a northeast (N25/30° E) trending system of smaller scale faults, comparing with the north–south trend is observed. An east–west-trending trough appears at 27.5° N latitude which shows a deflection towards the northeast around 260.5° E longitude. In this zone of deflection a system of faults is well developed, which has smaller dimensions, either by length and width, than the north–south trending grabens.

The stratigraphy of the area was defined by Scott and Tanaka (1986) within the framework of the regional mapping of the western hemisphere of Mars. Tanaka (1990) made some modifications that included: (1) differences in placement of contacts and amount of detail shown, (2) grouping of most units of the Alba Patera and Ceraunius Fossae Formations into Ahac unit, and (3) reassignment of some stratigraphic positions (i.e. HF unit). Plescia (2000) made a detailed study of Ceraunius and Uranius Tholi, defining different stratigraphic units based on morphological criteria (i.e. abundance of gullies and textures) found within each of the volcanic edifices. In order to have a geological framework we mainly followed the stratigraphic units defined by Tanaka (1990) and Plescia (2000) (Fig. 3).

2. History of faulting

Deformation in the region has a long-term history since Late Noachian until Amazonian (Borraccini et al., 2005). Most of the area is mainly affected by north–south faults, but also there is a large east–west depression to the north of the area, and some minor faults trending northeast–southwest. History of deformation began with the development of normal faults with N30° E strike (Phase 1) in the upper Noachian. Later it was followed by north–south faults of Phase 2 that propagated the deformation from west to east approaching the volcanic structures Ceraunius Tholus and Uranius Tholus, and reached the easternmost position during Phase 4, in the lowest part of the upper Hesperian. Finally, reactivation of the main faults possibly took place in a much later stage, during Early Amazonian (Fig. 4).

The fault system with northeast–southwest strike has been identified by Tanaka (1990) as an older event (Episode 1). The trend of these faults is correlated with other faults and structures of similar direction located in Tempe Terra, a region to the northeast of the study area. The faults of that region are of Noachian age on average, therefore, this same age is assigned to the faults with this direction in the study area (Tanaka, 1990). Taking into account that the older unit that is being cut by the faults in the study area is the Fractured Hesperian (HF) unit, of upper Noachian–lower Hesperian age, we propose to consider the beginning of the deformation as upper Noachian.

We have proposed different phases in the history of deformation: Phase 1 is equivalent to Episode 1 of Tanaka (1990). Nevertheless, as argued above, we here propose a younger, upper Noachian age for it since they cut HF unit, which is Late Noachian–Early Hesperian in age (Fig. 4a). A second phase of deformation (Phase 2), involves the development of a north–south fault system towards the west of the study area. It is observed that this system of faults predates the east–west trough (Fig. 5). Although the development of this phase cannot be restricted only to the west, active faulting may have ceased in the western sector of the study area earlier than in the East sector. In the eastern sector north–south faults cuts east–west depression while in western section north–south faults are been cut by the east–west depression (Fig. 5). Phase 2 is followed by the formation of the east–west graben located at 27.5° north latitude (Phase 3). There is rectangular orthogonal fault pattern around 261° E 27.5° S, associated with the east–west fault that would have been developed during this third phase due to a change in the direction of the stress from east–west to northwest-southeast (Fig. 4c). A similar system of orthogonal faults appears in Noctis Labyrinthus. Bistacchi et al. (2004) concluded that this particular geometry was a consequence of two orthogonal efforts that acted at the same time. Considering the direction of some of these small faults (∼N30E), they may have reactivated old structures generated during Phase 1. The main east–west oriented stress in the area would have continued acting during Phase 4, propagating the deformation to the East. These faults, located mainly in the central and eastern sector of the area, cut the principal east–west structure of Phase 3 (Fig. 4d). These three last phases, 2, 3 and 4, would be equivalent to Episode 2 proposed by Tanaka (1990). Finally, a reactivation of the main structures in a much younger stage Amazonian would have taken place. Evidence of this reactivation would be the association of these structures with the development of pit craters, considered among the youngest structures on Mars (Ferrill et al., 2004; Fig. 4e).

3. Measurements of the extension

Most of the structures in the area are simple grabens with a central trough flanked by two normal faults. The horizontal extension (Ex) between the hanging-wall block and foot-wall block of a normal fault can easily be determined from the structural relief generated by the fault (r) and its dip of the fault angle (α) (Golombek et al., 1996):

$$Ex = \frac{r}{\tan\alpha}. \quad (1)$$

In many cases, the original fault dip (α) cannot be measured because the original fault slope has been modified by secondary processes (e.g. mass wasting) or cannot be measured using MOLA topography (Smith et al., 2003) because, due to lower resolution of MOLA data, only points representing the hanging-wall and foot-wall elevations are sampled; the slope has to be derived from these points. The original normal faults, then, were considered to have an average dip angle of 60°, following Golombek et al. (1996) on the basis of mechanical arguments and the direct observation of the simple faults that bound grabens in the Moon and Mars. Taking this into account, the extension in the study area was calculated based on the difference of topographic relief between the hanging-wall and the foot-wall, according to Eq. (1). It was assumed that only normal slip took place, since there is no evidence of strike-slip displacement in this region (Borraccini et al., 2005). Three profiles were made at 25°, 26° and 27° of north latitude respectively, and we calculated the total extension for each profile as the sum of the individual heave values of each fault (Fig. 6). In order to interpret the geology correctly and to measure only those elevation differences that correspond to tectonic structures (i.e. normal faults), each topographic profile was compared with the MDIM 2.1 image (Kirk and Archinal, 2004), to give to the extension values a geologic significance. It was assumed that: (1) slopes lower than 60° correspond to faults affected by mass-wasting, and (2) where pit crater chains are located on faults, the relief generated by the fault, has been exaggerated by the formation of the pits (Fig. 7).

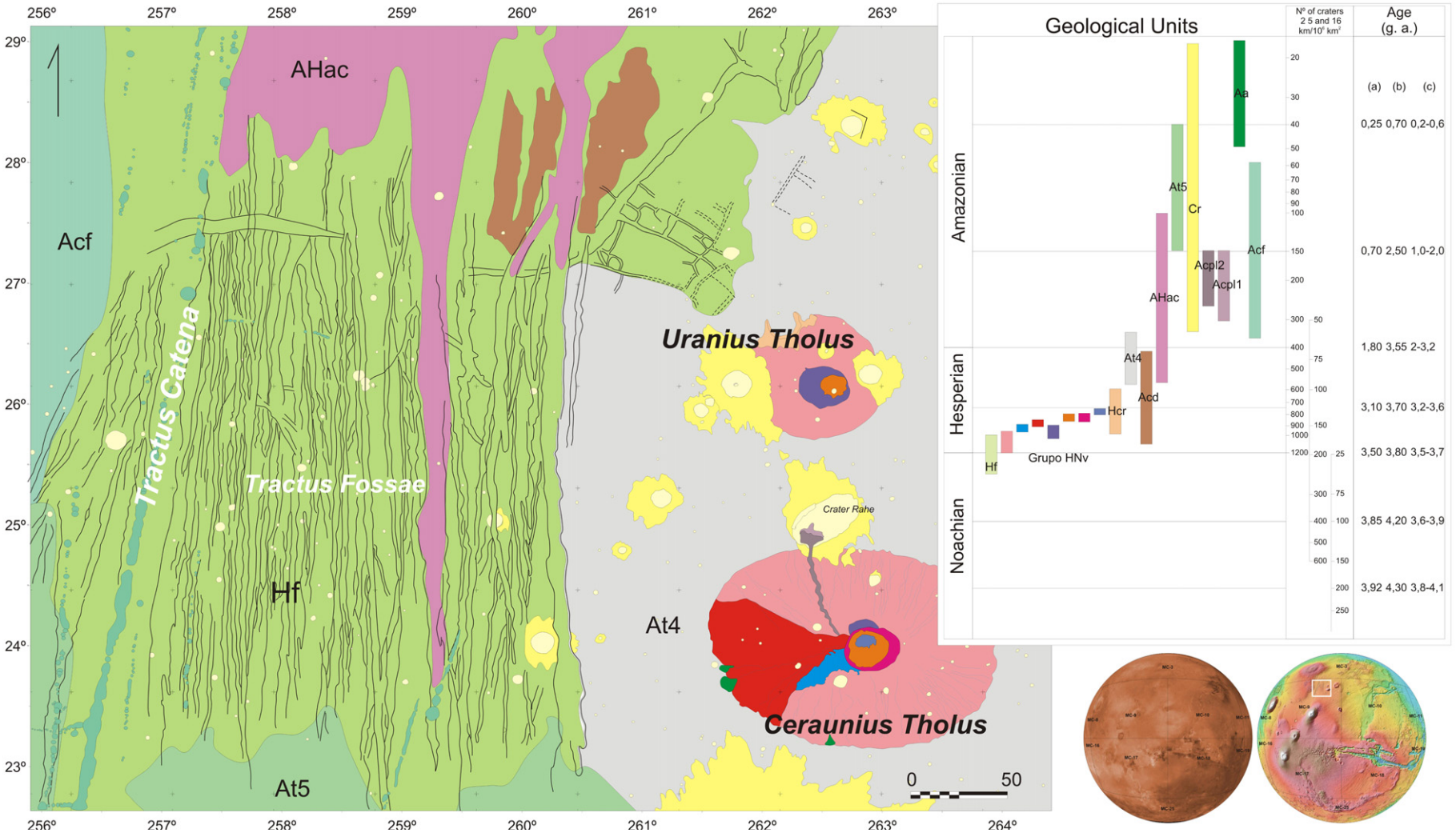

Fig. 3. Geologic sketch map of the study area, modified from Tanaka (1990) and Plescia (2000), showing morphological units and structures, together with the proposed ages of each unit to. It can be seen that fractured terrain and volcanic edifices both have lower Hesperian ages.

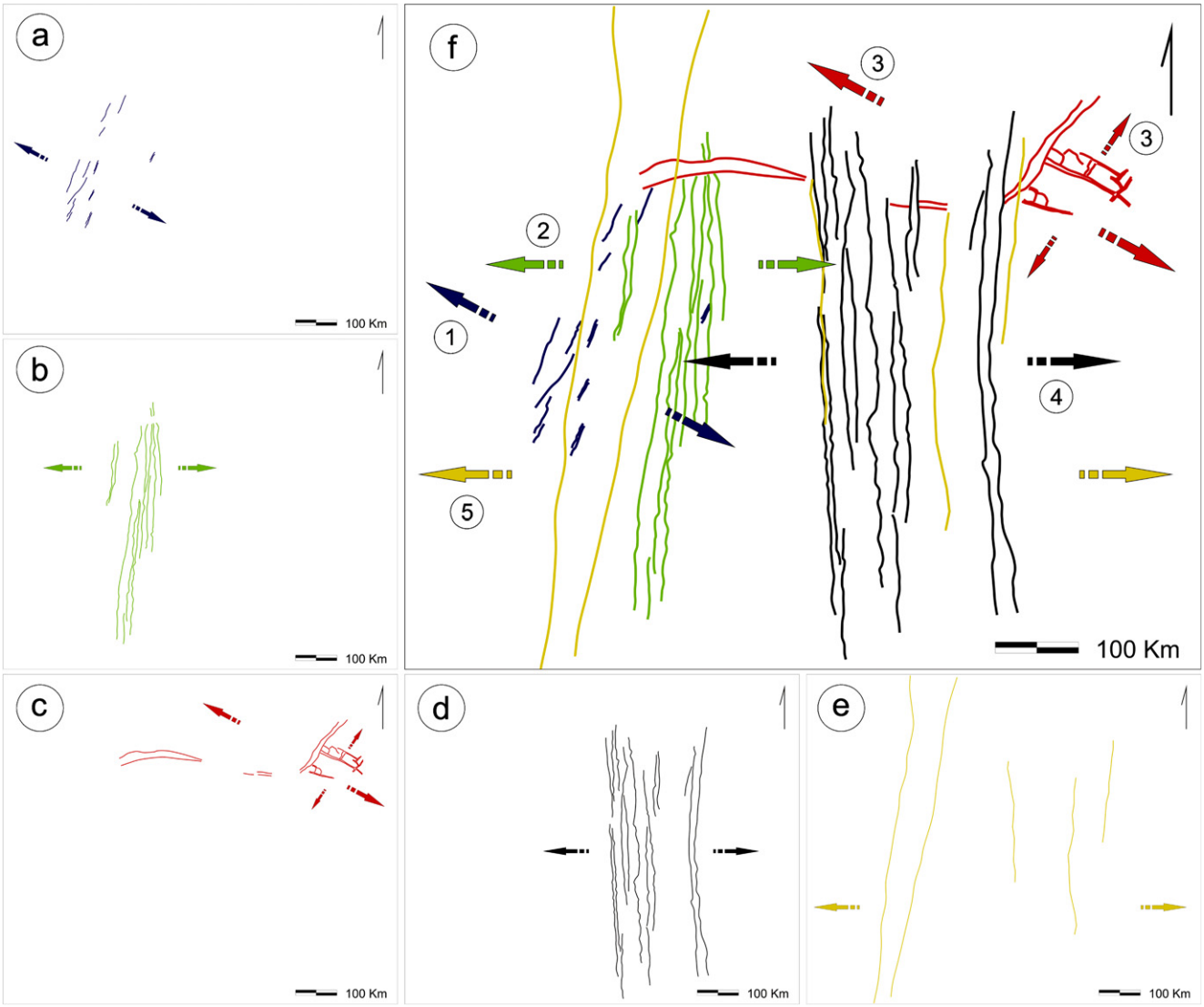

Fig. 4. Different stages of faulting: (a) Phase 1, upper Noachian; it is an early faulting that might be related with Tempe Fossae dynamics. (b) Phase 2, Noachian–Hesperian boundary; north–south faults begins to form in the western sector. (c) Phase 3, lower Hesperian; during this time a change in stress direction may occur producing the east–west depression. (d) Phase 4, upper Hesperian; stress regime returns to have an east–west direction. (e) Phase 5, Amazonian; young faulting related to pit crater chains.

Table 1
Total extension (km).

References	Latitude	Fault dips			
		60°	70°	80°	60°/80°
This work	25°	3.31	2.10	1.00	**3.00**
	26°	4.19	2.64	1.28	**3.89**
	27°	4.33	2.73	1.32	**4.18**
Borraccini et al. (2005)	26°			1.2	
	24°			9	
Hauber and Kronberg (2001)	Extension values for Tempe Fossae				2.5–5

Measurements of total extension for three different latitudes in the area compared with values from literature. The values are in kilometers and represent the sum of the extension from individual grabens for four different dip angles: 60°, 70°, 80° and the combination of 60° and 80°.

We obtained measurements of 161 individual normal faults, and calculated the extension for each of the profiles using four different dip angles. The calculations were made assuming fault dips of 60°, 70° and 80°, and a combination of 60° and 80° according to the geologic interpretation of the profile (Table 1). We used 80° of dip for the faults that were associated with pit crater chains and 60° for the well visible scarps. Values higher than 60 where used because of the uncertainties of real dip values, as was also proposed by Golombek et al. (1996) where he considered a mean value of 60° ± 15°, while the combination of 60° and 80° where based on interpretation of the profiles as can be seen in Fig. 7. These values were used in order to be as conservative as possible in the assessment of the extension and give minimum extension values.

The results differ remarkably from recent measurements by Borraccini et al. (2005). These authors obtained a value of 12 km of extension at 26° latitude and 9 km of extension at 24°. In this work we obtained 4.18 and 3 km of extension at 27° and 24° respectively. The differences in the values of extension are mainly related to the different interpretation of the study profiles. In their work, the deepest topographic depressions have been considered as grabens and, therefore, as the result of the extension only, which is the reason why these troughs (as it is the case of Tractus Fossae, that reaches up to 1 km of depth) add considerable values to the total amount of extension. In the present work, however, it is recognized that the depth of some grabens does not correspond to the movement of the blocks themselves, but it is a consequence of collapse processes by pit crater forma-

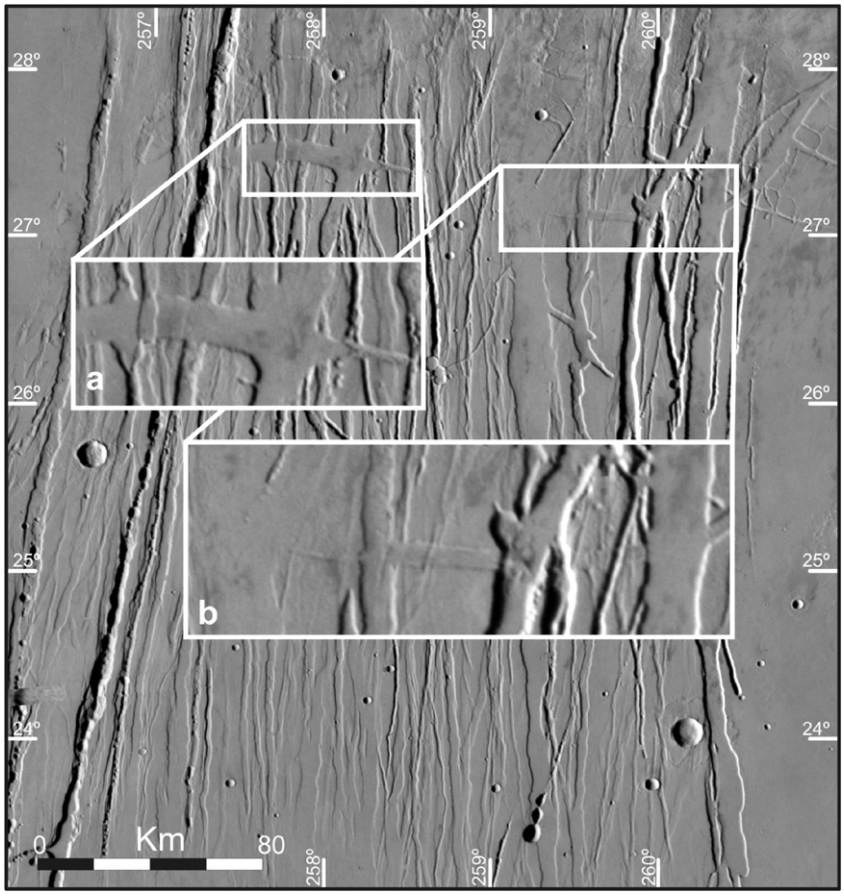

Fig. 5. MDIM 2.1 image showing a detail of crosscutting relation between faults. (a) shows that western faults are mainly affected by the E–W structure while (b) shows that most of the faults cut that structure.

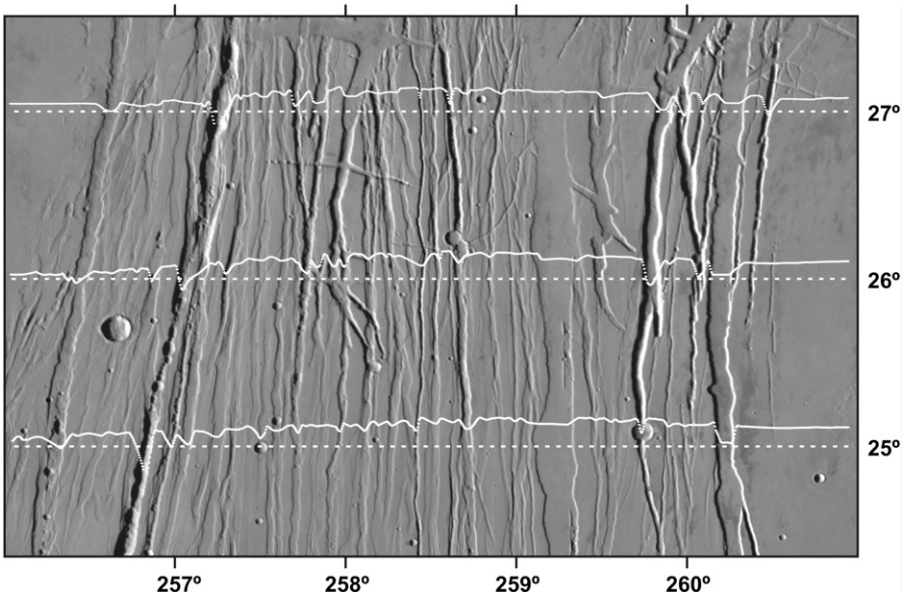

Fig. 6. Location of the three topographic profiles used to measure extension. Profiles are compared with MDIM 2.1 image in order to make an accurate interpretation of elevation differences.

tion as mentioned earlier. The values presented here are nothing but minimum estimates of extension because we do not discard the possibility of rotations due to listric fault geometry. The values are too high to be a consequence of uplifted flexure of the central part (Borraccini et al., 2005). Therefore, the calculated values of extension support the hypothesis of Tanaka (1990), who interpreted grabens as the expression of a system of regional extension. It is interesting, however, that in both studies the amount of extension is greater in the north than in the south, both with almost the same ratio, about 0.76. This fact could be implying that extension may have started at north and faults propagated towards the south.

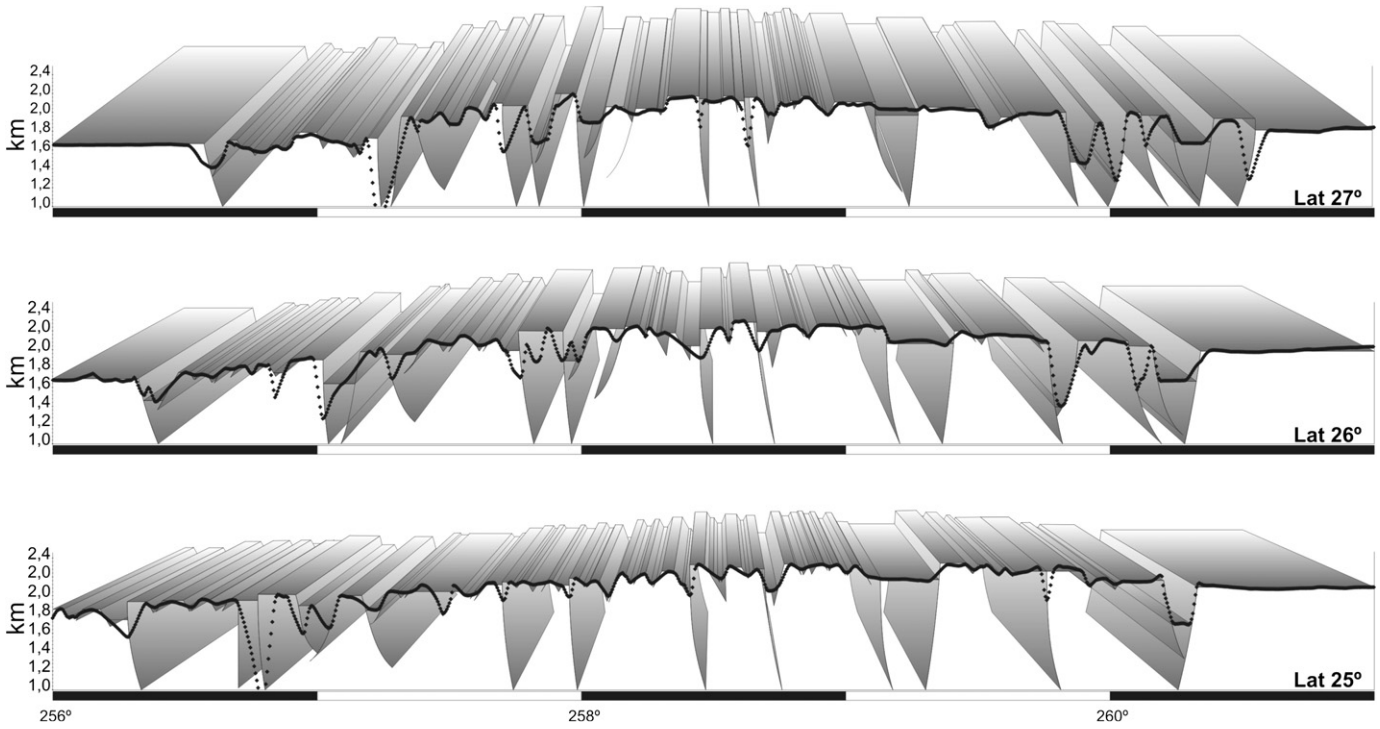

Fig. 7. The figure shows the Interpretation of topographic profiles from Fig. 6 using MOLA data (dots). Fault planes were drawn so that different dip angles could be used. Vertical scale is in kilometers.

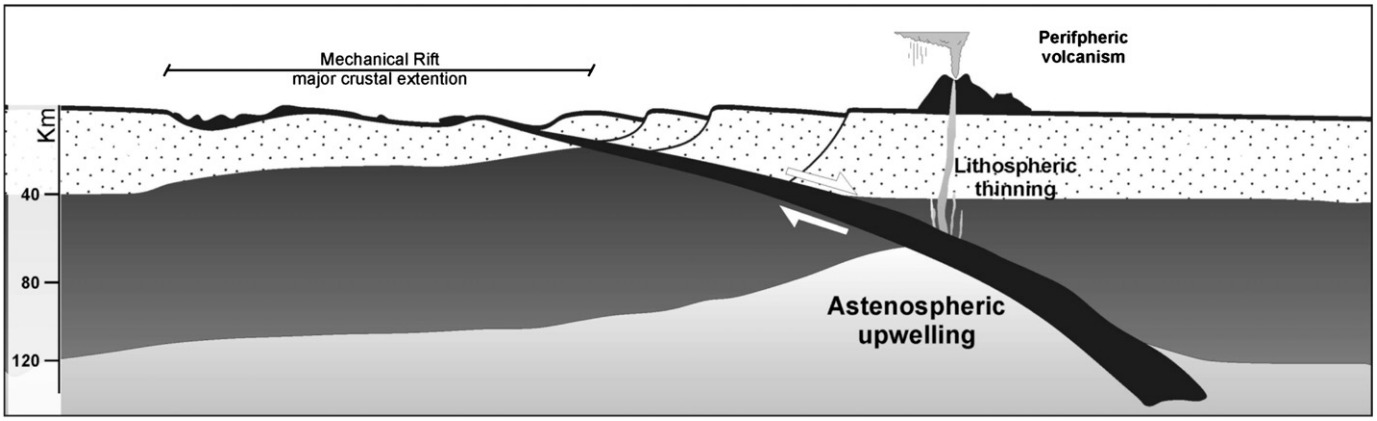

Fig. 8. Asymmetric rift model modified from Wernicke and Tilke (1989) showing upper plate with volcanic products in the right, just above the asthenospheric ascent material, and mechanical rift towards left.

4. Discussion: Asymmetric rift systems

Olsen and Morgan (1995) defined a continental rift as "an elongated tectonic depression associated with which the entire lithosphere has been modified in extension." The initiation of a rift system and the rupture of the continents are processes whose genesis is still under analysis and discussion, and its explanation gave rise to several models (Bellahsen et al., 2003). Although the generation of rifts is always associated with anomalously high thermal fluxes and the ascent of hot mantle material, the models that explain the dynamics of the process have changed through time. The first attempts to explain rifts used symmetrical, pure shear models (McKenzie, 1978), where the extensional structures formed exactly over the thermal anomaly. Discussions were focus on the relative roles of mantle ascent and crustal extension, if the ascent of the mantle material were forced during crustal extension or if it was all the other way around (Illies, 1981; Bott, 1982; Spohn and Schubert, 1982). Later, numerous regional seismic sections made in several continents showed that most of the rifts were asymmetric structures, as early proposed by Wernicke (1981).

Terrestrial asymmetric rift models, due to the increasingly observed subsurface evidence, were subsequently favored over symmetrical models. Asymmetric rifts models postulate peripheral volcanism in the early stage of evolution. In this model, given the inclination of the master shear zone in the simple shear deformation, the thermal signature associated with extension in the lower crust is offset from the zone of brittle deformation in the upper crust (Wernicke, 1981; Bosworth, 1985, 1987; Fig. 8). The Eastern African Rift is considered a classical model of continental rifts. This area is the most extensive zone of active rifting, and has concentrated a variety of geologic and geophysical studies (e.g. Mechie et al., 1997; Baker and Wohlenberg, 1971; Jestin et al., 1992). It is an asymmetric rift associated with the presence of one plume around northern Ethiopia, in the Afar triangle zone. The continuous magmatic activity, along with numerous volcanic centers throughout the rift and towards its flanks, was associated with the propagation of this

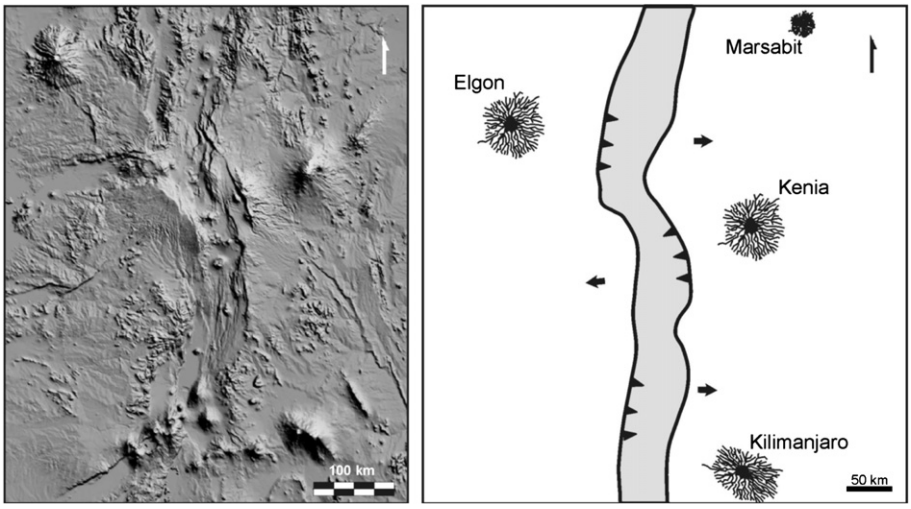

Fig. 9. Peripheral volcanism associated with the Gregory's rift. (Left) SRTM topography. (Right) Schematic draw of principal volcanoes, associated with crustal extension, located between 100 and 150 km away from central grabens.

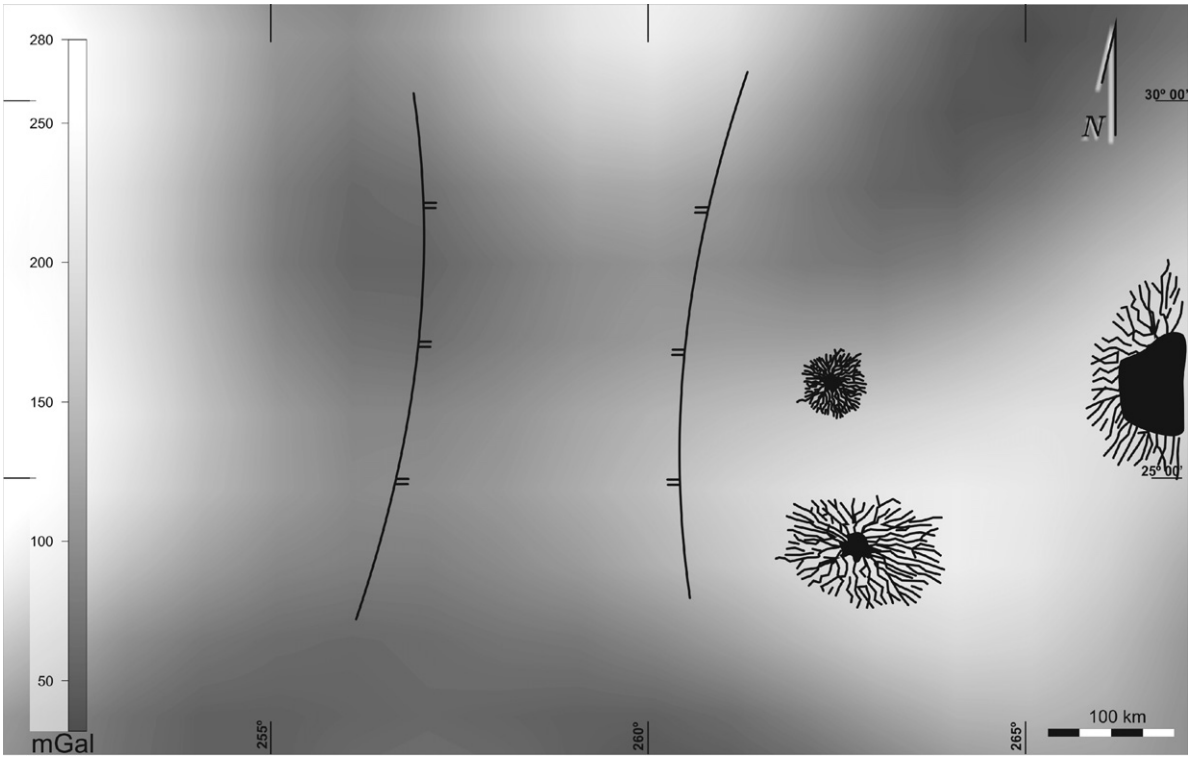

Fig. 10. Gravimetric anomalies in gray scale and the location of principal structures from the study area. Central deformed area is located in lower values while volcanoes edifices are just over gravimetric highs. The data is from GGM1025A product derived from MGM1025 model (Lemoine et al., 2001).

structure towards the south (Rosendahl et al., 1992; Morley, 1994; Mechie et al., 1997; Keller et al., 1994). Rift processes have been postulated several times for Mars and elongated extensional structures, like Tempe and Ceraunius Fossae, or Tantalus Fossae, have been related to them (Mutch and Saunders, 1976). But the one that has been more related and compared to a terrestrial continental rift is the Valle Marineris (Anderson and Grimm, 1998). Likewise, the region of Tempe Fossae was also compared with the Kenya Rift (Hauber and Kronberg, 2001).

Although the general dimensions East African Rift System are not comparable with the zone of Tractus Fossae, some important similarities indicate that these two regions could be similar in nature, and the processes that acted in both cases may have been comparable. Pioneering works from Bosworth (1987) in the Gregory rift showed the crucial relation between the off-axis volcanism and rift dynamics, a model that then became applicable to many other rift systems. A clear example of this are the volcanoes Kenya and Kilimanjaro, which are located between 100 and 150 km away from the main axis of the structural extension (Fig. 9). Other authors have also suggested that the greater lithospheric thinning would occur at certain distance from the superficial crustal extension (Wernicke, 1981). Similarly, in this study area we observe an analog spatial relation between volcanism and faulting, where Ceraunius Tholus and Uranius Tholus are located approximately 250 km to the east from the central faulting zone. There is also a temporal link between volcanism and graben formation. The stratigraphic interpretation, based on existing dating, shows that these volcanic centers and the first north–south faults

would have an upper Noachian-lower Hesperian age, and would be contemporary with the north–south fault system of proposed phases 2 and 4. Moreover, faulting and volcanism predate lava floods from unit At4 constraining the upper age of both events to lower Hesperian. Furthermore, it is known that the initial stage of the terrestrial rift system is dominated by polygenic off-axis magmatism with highly differentiated alkaline central volcanoes (Bosworth, 1987). Morphologic studies of Ceraunius Tholus and Uranius Tholus (Plescia, 2000) indicate that they could be polygenic central volcanoes, and that in their construction would have participated as many episodes of lavic effusions as pyroclastic sequences.

There is a wide positive gravimetric anomaly associated with the volcanic centers (Fig. 10). Given the age of the volcanic centers, it is improbable that this anomaly responds to present dynamic processes, like plumes. One potential implication of this anomaly is that this zone was not only subject to lithospheric thinning, but also to underplating processes and emplacement of subsurface mafic bodies (intrusions). This mechanism has been proposed, for example, for the opening of the Red Sea (Ghebreab, 1998). The intrusion of asthenospheric material at low levels would have left a relic zone of greater density near the surface, generating the observed regional positive gravimetric anomaly.

Seismic sections across many terrestrial rift systems are characterized by asymmetric grabens or half-grabens, which in many cases are dominated by listric faults (Chorowicz, 2005). In the case of Tractus Fossae it is not possible to directly observe the deeper structure; however, considering the geometry of terrestrial rifts, three sections were done in order to calculate extension values on a geologic framework. Although some authors have considered the possibility of rotations unlikely (Borraccini et al., 2005), the topographic profiles presented here may reveal blocks tilting. An elevation difference exists between the surrounding plains and the center of the graben zone. When regional blocks are considered in topographic profiles it can be seen that some of them might be tilted. This, together with variable offset along graben bounding normal fault could be evidence that big blocks would be slightly rotated (Fig. 11). Moreover, if pit craters are associated with deep faults, the main structure would consist of listric faults related to a detachment fault reflecting lithospheric thick-skinned deformation down to a brittle–ductile transition (Schultz et al., 2007). Total extension calculated in the southern part of East African rift, which corresponds to the initial stage of the system, varies between 5 and 10 km. In the study area, the calculated average extension was 4 km. As mentioned before, this value of extension would be minimum and are consistent with a model of an initial phase of rift systems but high enough to be related with horizontal movements and not with bulging. There are also variable extension values along strike, being higher at north section, which is also in agreement with variable extension along rifts related with time dependence aperture.

The relations studied between the volcanism and the faulting indicate that both would have begun at the same time, and that magmatism would have been developed in a peripheral zone with respect to the axis of main fracture zone, in similar way to the Kilimanjaro volcano and East African rift. In both cases the volcanoes would be located directly over the thermal anomaly and maximum lithosphere attenuation. In the study area, volcanoes Ceraunius Tholus and Uranius Tholus would represent the peripheral volcanism above the asthenospheric anomaly that accompanied the structural extension to the west. The fault system would be dominated by an inclined master fault dipping to the east. This detachment zone is proposed here to reach a depth of nearly 45 km, which is the mean crust thickness for this area (Zuber et al., 2000). Although 45 km is the mean crustal thickness today, we think that is a good approximation considering that main tectonic

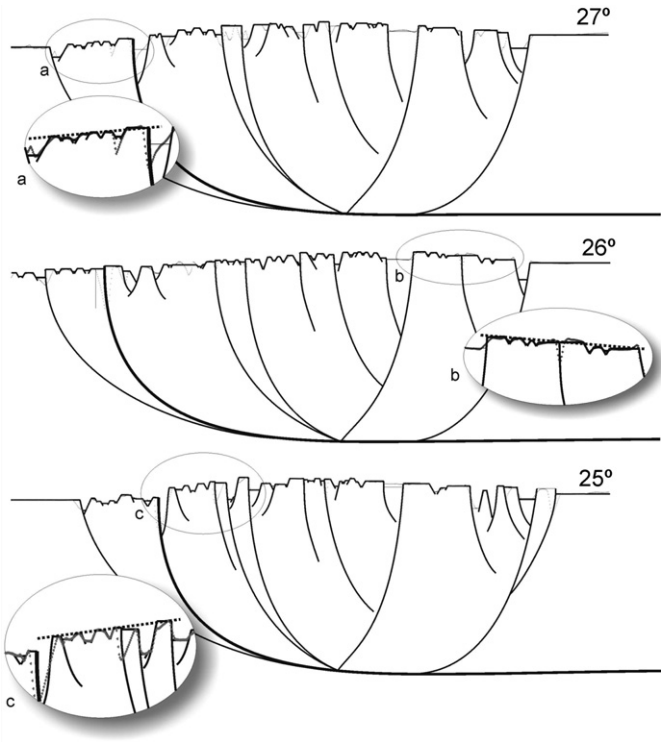

Fig. 11. Interpretation of topographic profiles based on the analogy with terrestrial rift geometries. Listric faults were located under pit craters, considering that for the formation of that structures faults starts as vertical tension cracks and progressively change the angle as get deep. (a), (b) and (c) show detail sections of profiles where blocks might have undergone some rotation. In many cases that coincides with the presence of proposed listric faults.

activity in Mars lasted until ~3.5/3.1 G.a. After it was fossilized in that period it should not have change severely, since there weren't any stacking or stretching event. Moreover, Hauber and Kronberg (2005) also proposed that in Thaumasia region the faults should have listric geometry and by geometrical parameters they arrived to the conclusion that a possible listric master fault should be between 66.7 and 33.3 km deep.

Finally, the Tractus Fossae region would have evolved like an asymmetric rift system. Considering the low extension values we propose that rifting was aborted in an incipient stage were the thermal anomaly did not reach the mechanical rift (Fig. 12).

5. Geologic history

1. During the lower and middle Noachian, the crust and associated lava flows constitutes the unit HF (Figs. 13a and 13b).
2. Towards the end of the upper Noachian the deformation in the area would have begun with the generation of N30° E-trending grabens (phase 1), preceding (peripheral) volcanism (Figs. 13c and 13d).
3. In the Noachian–Hesperian limit we document the onset of volcanism east of the region with the generation of the Ceraunius Tholus and Uranius Tholus while, in the west, phase 2 of faulting started. These two events would have been consequence of thermal anomaly underneath the volcanic bodies, analogous to terrestrial rift systems.
4. During lower Hesperian north–south fault propagated towards the east during phase 4 of deformation (Fig. 13f).
5. Volcanic activity in the area would have ended during lower Hesperian.
6. Lavas of the AHcf unit partially infill the area, from north to south, during lower Amazonian or upper Hesperian. Evidence of some faults cutting this unit would indicate that phase 4

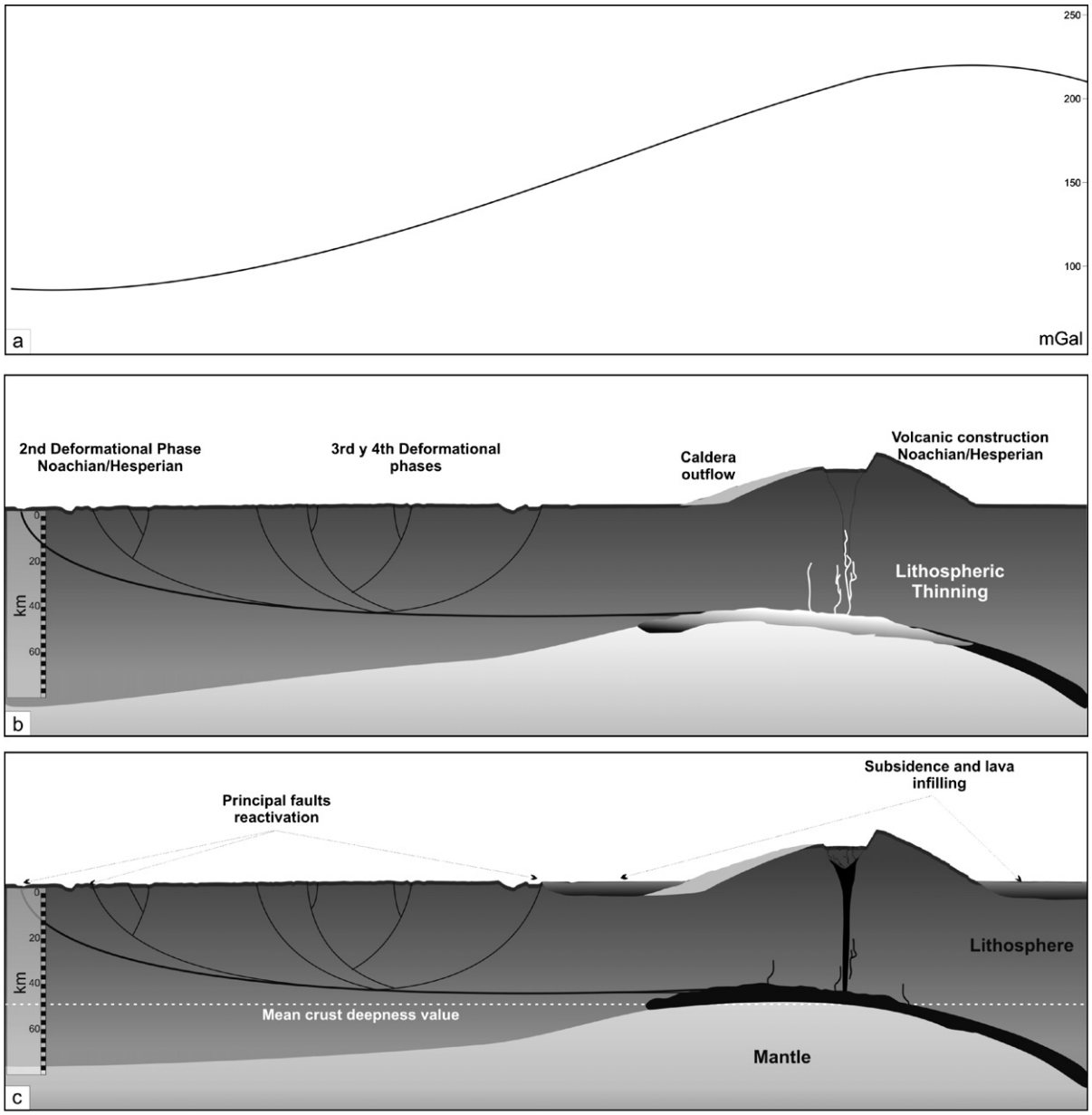

Fig. 12. Final model and evolution of the area as an asymmetric rift system. (a) Gravity anomaly profile that shows correlation between high values and volcanoes location. (b) Asthenospheric upwelling would have triggered first deformation stages and volcanism. (c) After the system cooled down, subsidence affected eastern section and some faults were reactivated.

would have extended until the beginning of the upper Hesperian (Fig. 13g).

7. After the end volcanic activity the area would have went through a thermal subsidence (Fig. 13h).
8. Later on, lava flows flooded the depressed region, generating At4 unit (Figs. 13i and 13j).
9. During Amazonian two lava units would have entered to the zone, Acf and At5, from the northwest and the south of the region respectively (Figs. 13k and 13l).
10. Finally, a reactivation of the main faults, demonstrated by the generation of the pit crater chains, would have occurred at the middle to upper Amazonian limit, during phase 5 deformation.

6. Conclusions

After emplacement of lava flows during lower Noachian volcanism at the east of the region together with faulting started during Noachian–Hesperian boundary. These two events would have been consequence of thermal anomaly underneath the volcanic bodies. Later on this activity ended during lower Hesperian and the area was partially filled by lava flows during Amazonian. By this time some faulting occurred, probably by accommodation of previous faults, which generated pit crater chains.

Cross-sectional asymmetry may be the rule and not the exception at lithospheric scale on Earth (Wernicke and Tilke, 1989). Based on that, we here proposed that Tractus Fossae region might have evolved as an asymmetric rift. Evidences of that include: the spatial relation between faulting and volcanism; the temporal relation constrained by stratigraphic units; that main phases of activity of faults and volcanoes not only have started, but also ended at similar times; the gravimetric anomalies and history and mechanics of faulting; type of volcanism, which shows polygenic central off-axis volcanoes typical from incipient terrestrial rifts. As mentioned in Section 3, values of extension are high enough to be consequence of regional horizontal extension, which may be related to the nearby thermal anomaly underneath Ceraunius Tholus

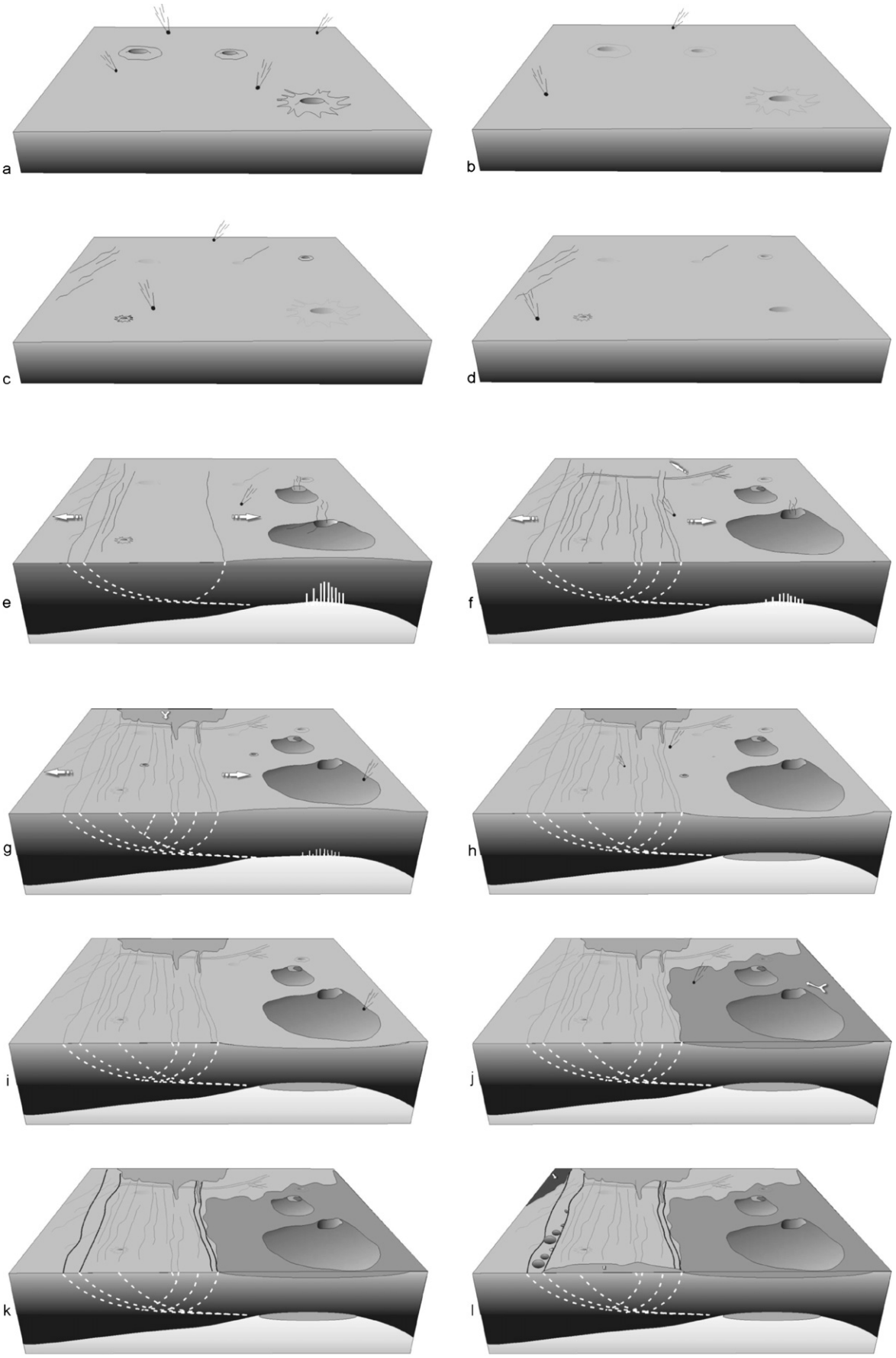

Fig. 13. Evolution of the study area: (a and b) lower and middle Noachian; (c and d) upper Noachian; (e) Noachian–Hesperian; (f) lower Hesperian; (g) Hesperian–Amazonian; (h and i) thermal subsidence; (j and k) lower Amazonian; (l) middle Amazonian.

and Uranius Tholus. However, values of extension are low and are in the order those from incipient Central Kenya rift. Moreover, there is no evidence that thermal anomaly reached the mechanical rift. Based on that we propose that rifting was aborted in an incipient stage.

Tractus Fossae region is located South–East of Alba Patera volcanic center, which may be the consequence of a large plume (Cailleau et al., 2005). We showed that extension values are higher in the north than in the south indicating that rifting may have propagated from north to south. Formation of the rift in a propagating manner is energetically preferred, as it requires less total driving force than if the rift were to be formed simultaneously along its entire length (Kiefer and Swafford, 2006; Parmentier and Schubert, 1989). Similar to East African rift which has started in the Afar Triangle and propagated towards the south, Tractus Fossae rifting process may have been a consequence of the active plume in Alba Patera together with thermal anomalies located immediately to the north. Relationships between faults and volcanism require further examination that could be done in near future using increasingly Mars data-set like SHARAD or MARSIS for subsurface observations and HIRISE images to evaluate more properly the cross cutting relations and fault ages.

Acknowledgments

We are grateful for the thoughtful reviews of Ernst Hauber and an Anonymous reviewer whose insightful comments and suggestions resulted in a greatly improved manuscript. We also would like to particularly acknowledge Ernesto Cristallini and Angelo Pio Rossi for the useful comments and discussions.

Appendix A. MOC narrow angle images (Malin et al., 2007)

Number of image	Description
m0202085	Floor of trough in Tractus Fossae with many small pits
m0204872	Upper surface in Tractus Fossae area
m0306621	Sample a trough in the Tractus Fossae
m0800606	Sample troughed terrain of Ceraunius Fossae
m0801927	Cross pitted trough in Ceraunius Fossae
m0807466	Sample terrain in Tractus Catena
m1202749	Sample
m1301207	Sample
m1402069	Rectilinear troughs NW of Uranius Tholus
m1501055	Crater and pitted trough in Ceraunius Fossae region
m1501659	Ceraunius Tholus contact between lower NW flank and plains
m1600696	Ceraunius Fossae trough sample
m1800353	Pits/troughs in Ceraunius Fossae
m1900204	Cross rectilinear troughs NW of Uranius Tholus
m1901108	Sample troughs/graben in Tractus Fossae terrain
m2000723	Cross deep trough in Tractus Fossae terrain
m2001180	Ceraunius Fossae sample
m2100185	Sample large trough in Tractus Catena region
m2100338	Contacts between two impact craters and ejecta from another
m2101128	Tractus Fossae sample
m2301438	Sample trough in Tractus/Ceraunius Fossae region
e0100446	Cross troughs in Ceraunius Fossae
e0202159	Chain of pits in graben in Ceraunius Fossae
e0503255	Pits on valley floor in Tractus Fossae
e0902265	Ceraunius Fossae survey traverse
e1000369	Contact between plains and Tractus Fossae terrain
e1000370	Pit in trough in northwest Tractus Fossae
e1001858	Tractus Fossae survey
e1200378	Pits in Tractus Catena/Ceraunius Fossae region
e1200613	Traverse across western Ceraunius Tholus
e1300896	Contact between plains and Tractus Fossae ridges/troughs
e1301113	Traverse across lower west flank of Ceraunius Tholus
e1301747	Sample northeastern Tractus Fossae pits
e1500491	Terrain sample north of Tractus Catena

References

Anderson, S., Grimm, R.E., 1998. Rift processes at the Valles Marineris, Mars: Constraints from gravity on necking and rate-dependent strength evolution. J. Geophys. Res. 103, 11113–11124.

Anderson, R.C., Dohm, J.M., Golombek, M.P., Haldemann, A.F.C., Franklin, B.J., Tanaka, K.L., Lias, J., Peer, B., 2001. Primary centers and secondary concentrations of tectonic activity through time in the western hemisphere of Mars. J. Geophys. Res. 106, 20563–20585.

Anderson, R.C., Dohm, J.M., Haldemann, A.F.C., Hare, T.M., Baker, V.R., 2004. Tectonic histories between Alba Patera and Syria Planum, Mars. Icarus 171, 31–38.

Baker, B.H., Wohlenberg, J., 1971. Structure and evolution of the Kenya Rift Valley. Nature 229, 538–542.

Bellahsen, N., Faccenna, C., Funiciello, F., Daniel, J.M., Jolivet, L., 2003. A kinematic model of the Afar depression and its paleogeographic implications. Earth Planet. Sci. Lett. 216, 383–398.

Bistacchi, N., Massironi, M., Baggio, P., 2004. Large scale fault kinematic analysis in Noctis Labyrinthus (Mars). Planet. Space Sci. 52, 215–222.

Borraccini, F., Lanci, L., Wezel, F.C., Baioni, D., 2005. Crustal extension in the Ceraunius Fossae, Northern Tharsis Region, Mars. J. Geophys. Res. 110, doi:10.1029/2004JE002373. E06006.

Bosworth, W., 1985. Geometry of propagating continental rifts. Nature 316, 625–627.

Bosworth, W., 1987. Off axis volcanism in Gregory rift, East Africa: Implications for models of continental rifting. Geology 15, 397–400.

Bott, M.H.P., 1982. Origin of the lithospheric tension causing basin formation. Philos. Trans. R. Soc. London A 305, 319–324.

Cailleau, B., Walter, T.R., Janle, P., Hauber, E., 2005. Unveiling the origin of radial grabens on Alba Patera volcano by finite element modeling. Icarus 176, 44–56.

Carr, M.H., 1974. Tectonic and volcanism of the Tharsis region of Mars. J. Geophys. Res. 79, 3943–3949.

Carr, M.H., 1975. Geologic map of the Tharsis Quadrangle of Mars. United States Geological Survey. Miscellaneous Investigation Series Map I-893.

Carr, M.H., Masursky, H., Saunders, R.S., 1973. A generalized geologic map of Mars. J. Geophys. Res. 78, 4031–4036.

Chorowicz, J., 2005. The East African rift system. J. Afr. Earth Sci. 43, 379–410.

Ferrill, D.A., Morris, A.P., Wyrick, D., Sims, D.W., Franklin, N.M., 2004. Dilational fault slip and pit chain formation on Mars. GSA Today 14 (10). 4-2.

Ghebreab, W., 1998. Tectonics of the Red Sea region reassessed. Earth Sci. Rev. 45, 1–44.

Golombek, M.P., Tanaka, K.L., Franklin, B.J., 1996. Extension across Tempe Terra, Mars, from measurements of fault scarp widths and deformed craters. J. Geophys. Res. 101, 26119–26130.

Greeley, R., Spudis, P.D., 1981. Volcanism on Mars. Rev. Geophys. Space Phys. 19, 13–41.

Hauber, E., Kronberg, P., 2001. Tempe Fossae, Mars: A planetary analog to terrestrial continental rift? J. Geophys. Res. 106, 20587–20602.

Hauber, E., Kronberg, P., 2005. The large Thaumasia graben on Mars: Is it a rift? J. Geophys. Res. 110, doi:10.1029/2005JE002407. E07003.

Hodges, C.A., Moore, H.J., 1994. Atlas of Volcanic Landforms on Mars. United States Geological Survey Professional Papers, vol. 1534. Geological Survey, Washington, DC.

Illies, J.H., 1981. Mechanism of graben formation. Tectonophysics 73, 249–266.

Jestin, F., Huchon, P., Gaulier, J.M., 1992. The Somalia plate and East Africa rift system: Present day kinematics. Geophys. J. Int. 116, 637–654.

Keller, G.R., Prodehl, C., Mechie, J., Fuchs, K., Khan, M.A., Maguire, P.K.H., Mooney, W.D., Achauer, U., Davis, P.M., Meyer, R.P., Braile, L.W., Nyambok, I.O., Thompson, G.A., 1994. The East African rift system in the light of KRISP 90. Tectonophysics 236, 465–483.

Kiefer, W.S., Swafford, L.C., 2006. Topographic analysis of Devana Chasma, Venus: Implications for rift system segmentation and propagation. J. Struct. Geol. 28, 122144–122155.

Kirk, R.L., Archinal, B.A., 2004. MDIM 2.1: Mars Global Digital Image Mosaic. US Geological Survey, Flagstaff, AZ. URL: http://astrogeology.usgs.gov/Projects/MDIM21/ (last date accessed: 24 February 2006).

Lemoine, F.G., Neumann, G.A., Chinn, D.S., Smith, D.E., Zuber, M.T., Rowlands, D.D., Rubincam, D.P., Pavlis, D.E., 2001. Solution for Mars geophysical parameters from Mars Global Surveyor tracking data. Eos (Fall Suppl.) 82 (47). Abstract P42A-0545, F721.

Malin, M.C., Edgett, K.S., Davis, S.D., Caplinger, M.A., Jensen, E., Supulver, K.D., Sandoval, J., Posiolova, L., Zimdar, R., 2007. MOC. Malin Space Science Systems Mars Orbiter Camera Image Gallery. http://www.msss.com/moc_gallery/.

McKenzie, D.E., 1978. Some remarks on the development of sedimentary basins. Earth Planet. Sci. Lett. 40, 25–32.

Mechie, J., Prodehl, C., Keller, G.R., Khan, M.A., Achauer, U., Gaciri, S.J., 1997. A model for the structure, composition, and evolution of the Kenya Rift. Tectonophysics 278, 95–119.

Morley, C.K., 1994. Interaction of deep and shallow processes in the evolution of the Kenya Rift. Tectonophysics 236, 81–91.

Mutch, T.A., Saunders, R.S., 1976. The geologic development of Mars: A review. Space Sci. Rev. 19, 3–57.
Olsen, K.H., Morgan, P., 1995. Introduction: Progress in understanding continental rifts. In: Olsen, K.H. (Ed.), Continental Rifts: Evolution, Structure, Tectonics. Elsevier, New York, pp. 3–26.
Parmentier, E.N., Schubert, G., 1989. Rift propagation. Geophys. Res. Lett. 16, 183–186.
Plescia, J.B., 1991. Graben and extension in Northern Tharsis, Mars. J. Volcanol. Geothermal Res. 96, 18883–18895.
Plescia, J.B., 2000. Geology of the Uranius Group volcanic constructs: Uranius Patera, Ceraunius Tholus, and Uranius Tholus. Icarus 143, 376–396.
Plescia, J.B., Saunders, R.S., 1982. Tectonic history of the Tharsis region, Mars. J. Geophys. Res. B 12 (87), 9775–9791.
Rosendahl, B.R., Kilembe, E., Kaczamarick, K., 1992. Comparison of the seismic reflection data. Tectonophysics 213, 235–256.
Schultz, R.A., Moore, J.M., Grosfils, E.B., Tanaka, K.L., Mège, D., 2007. The Canyonlands model for planetary grabens: Revised physical basis and implications. In: Chapman, M. (Ed.), The Geology of Mars: Evidence from Earth-Based Analogs. Cambridge University Press, Cambridge, pp. 371–399.
Scott, D.H., Tanaka, K.L., 1986. Geologic map of the western equatorial region of Mars. United States Geological Survey Miscellaneous, Investigation Series Map I-1802-A. Scale 1:15.000.000.
Scott, D.H., Schaber, G.G., Horstman, K.C., Dial, A.L., 1981. Map showing lava flows in the northeast part of the Tharsis Quadrangle of Mars. US Geological Survey Miscellaneous Investigation Series Map I-1267.
Smith, D.E., Zuber, M.T., Solomon, S.C., Phillips, R.J., Head, J.W., Garvin, J.B., Banerdt, W.B., Muhleman, D.O., Pettengill, G.H., Neumann, G.A., Lemoine, F.G., Abshire, J.B., Aharonson, O., Brown, C.D., Hauck, S.A., Ivanov, A.B., McGovern, P.J., Zwally, H.J., Duxbury, T.C., 1999. The global topography of Mars and implications for surface evolution. Science 284, 1495–1503.
Smith, D., Neumann, G., Arvidson, R.E., Guinness, E.A., Slavney, S., 2003. Mars Global Surveyor Laser Altimeter Mission experiment gridded data record. NASA Planetary Data System, MGS-M-MOLA-5-MEGDR-L3-V1.0.
Spohn, T., Schubert, G., 1982. Convective thinning of the lithosphere: A mechanism for the initation of continental rifting. J. Geophys. Res. 87, 4669–4681.
Tanaka, K.L., 1986. The Stratigraphy of Mars. J. Geophys. Res. 91 (B13), E139–E158.
Tanaka, K.L., 1990. Tectonic history of the Alba Patera–Ceraunius Fossae region of Mars. Proc. Lunar Sci. Conf. 20, 515–523.
Wernicke, B., 1981. Low-angle normal faults in the Basin and Range province: Nappe tectonics in an extending orogen. Nature 291, 645–648.
Wernicke, B., Tilke, P.G., 1989. Extensional tectonics framework of the US Central Atlantic Passive Margin. In: Tankard, A.J., Balkwill, H.R. (Eds.), Extensional Tectonics and Stratigraphy of the North Atlantic Margins. In: AAPG Memoirs, vol. 46, pp. 7–21.
Zuber, T.M., Solomon, S.C., Phillips, R.J., Smith, D.E., Tyler, G.L., Aharonson, O., Balmino, G., Banerdt, W.B., Head, J.W., Johnson, C.L., Lemoine, F.G., McGovern, P.J., Neumann, G.A., Rowlands, D.D., Zhong, S., 2000. Internal structure and early thermal evolution of Mars from Mars Global Surveyor topography and gravity. Science 287, 1788–1793.